A MOTION CONTROL AND OBSTACLE AVOIDANCE ALGORITHM FOR HYPER-REDUNDANT MANIPULATORS

Chau-Chang Wang* , Vijay Kumar** and Guay-Ming Chiu*

*Institute of Undersea Technology, National Sun Yat-sen University
70 Lian-Hae Road, Kaohsiung, Taiwan, ROC
E-mail:chauwang@athena.iut.nsysu.edu.tw
**General Robotics and Active Sensory Perception (GRASP) Laboratory,
University of Pennsylvania
3401 Walnut Street, Room 301C, Philadelphia, PA 19104-6228, USA

Abstract- To carry inspection or repair work in clustered environments, such as a ship wreckage, conventional non-redundant or mildly redundant manipulators may suffer from unavoidable collision with obstacles. Inspired by the manipulation of "elephant trunks" and the motion of "snakes", the idea of hyper-redundancy is introduced to solve this problem. The term "hyper-redundancy" refers to redundant manipulators with a very large number of degrees of freedom. In addition to the degrees of freedom needed to achieve major tasks specified for the end-effector, the rest of the degrees of freedom, or hyper-redundancy, can be used to carry out secondary tasks or to meet constraints imposed by the environment. This paper presents a artificial conservative field method which integrates inverse kinematics with obstacle avoidance so that obstacle avoidance can be done online. It treats manipulators as elastic structures carrying electric charges, and obstacles as point charges or line charges. Potential energy flows between these systems will drive manipulators to a state of equilibrium which all manipulator links stay away from all obstacles as far as possible. Another by-product of this method is the repeatability of kinematics solutions if no singularities are met. A formulation is given with examples to illustrate this approach.

1 INTRODUCTION

A manipulator is considered to be redundant if the number of degrees of freedom exceeds the dimension of the task space. Let the kinematic map relating the joint displacements, $q = (q_1, q_2, ..., q_n)^T$, and the end-effector displacement, x, be given by

$$x = f(q) \tag{1}$$

where q is the $n \times 1$ vector of joint displacements and x is a $m \times 1$ vector of coordinates that describe the end-effector position and orientation. We assume that f is smooth and differentiable up to second order in the whole work space. The manipulator is considered to be redundant if $n > m$. When n is much large m, it is further classified as a hyper-redundant manipulator.

Much research has been done on the problem of obstacle avoidance with either stationary or moving objects for redundant manipulators [9, 4, 5, 1, 6, 3]. Generally, this problem is solved either in motion planning level [2, 3], or in motion control level [9, 4]. In the former approach, the workspace and the paths have to be precisely specified. Therefore, it is limited to operation in a time-invariant environment. In the latter approach, the method of artificial potential field is widely adopted. In this method, various forms of artificial potential field are used to provide an distance-dependent repulsive force between manipulator links and obstacles.

It is well known that inverse kinematics obtained by using pseudo-inverse suffers from non-repeatability of solutions. In [8], they overcome this problem by modeling each joint with a user-prescribed stiffness/compliance function such that the manipulator behaves like an elastic articulated chain. It is referred as impedance-based repeatable control scheme for redundant manipulators. Since the manipulator is modeled as an elastic articulated chain, it will also take the form of a potential field in joint space. Inspired by this, we have the idea of integrating the impedance-based control scheme with artificial potential field obstacle avoidance. The remaining of this paper is organized as followings. First we re-formulate the impedance-based control scheme as a optimization problem. A simple point charge obstacle model is presented to illustrate how obstacle avoidance can be integrate into motion controllers. A couple of obstacle avoidance scenarios are tested to show the efficacy of this approach. Discussions and conclusions are presented in the last section.

2 Problem Formulation

2.1 Impedance-Based Pseudo-Inverse

We follow the approach of Mussa-Ivaldi and Hogan [8] which models the manipulator as an elastic structure (rigid links and elastic joints.)[11] Therefore, commanding the manipulator is equivalent to applying a fictitious force at the end-effector to make it deflect to the desired position. Since it is an elastic structure, when reaching equilibrium state, the manipulator will assumes a configuration which locally minimizes the potential energy stored in the system. Assume that the *ith* joint is linear elastic and takes the form of stiffness as:

$$Q_i = K_i(q_i - q_{0i}), \tag{2}$$

where Q_i, K_i and q_{0i} is the generalized force, stiffness, and relaxation angle of the joint respectively. The potential energy, $V(q)$, of the system can be expressed as:

$$V(q) = \frac{1}{2}(q - q_0)^T K(q - q_0) \tag{3}$$

where K is a matrix joint stiffness. Because the system is elastic, and q_i's are the generalized coordinates (and Q_i's the corresponding generalized forces), without loss of generality, we can assume that K is symmetric and positive definite.

If x is the desired end-effector position, the configuration at this position is the solution of the following minimization problem:

$$\min_q \frac{1}{2}(q - q_0)^T K(q - q_0), \; s.t. \; x = f(q) \tag{4}$$

A necessary condition for equilibrium is obtained by considering the stationary points of the function $\Psi(q) = V(q) + \lambda^T(x - f(q))$, where λ is a vector of multipliers. By setting $\frac{\partial \Psi}{\partial q}$ to zero we obtain:

$$\begin{aligned} K^T(q - q_0) - (\frac{\partial f}{\partial q})^T \lambda &= 0 \\ K^T(q - q_r) &= J^T \lambda \\ Q &= J^T \lambda \end{aligned} \tag{5}$$

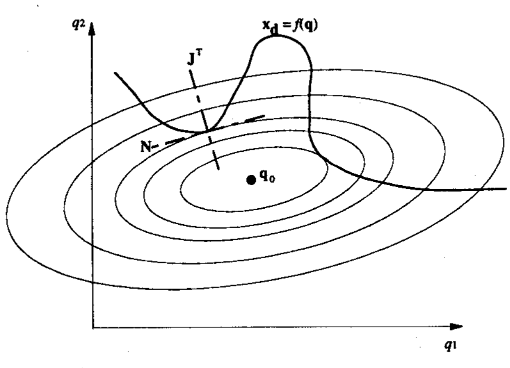

Figure 1: Minimum potential energy along a self-motion manifold.

λ is easily seen to be the the $m \times 1$ end-effector forces that must act on the end-effector for equilibrium.

For a given x in task space, the minimization problem in Equation (4) has a solution that is schematically represented in Figure 1. Note that the representation is strictly valid only for a two-dimensional joint space and a one-dimensional task space. However it is representative of the more general case when q is $n \times 1$ and x is $m \times 1$. Each contour (surface) describes configurations which have the same potential energy. The curve $x = f(q)$ is the self motion manifold for the manipulator. The gradient of the kinematic function, $f(q)$, is given by the transpose of the Jacobian and its direction is indicated in the figure. N is the null space at any point and its direction is orthogonal to J^T. A condition of equilibrium occurs when the gradient of the potential function belongs to the row space of the Jacobian matrix. At this point the null space vectors are tangential to the (convex) equi-potential surface, and motion along the self-motion manifold away from the point of tangency will only increase (or only decrease) the potential energy. the following $2n + m$ equations in $q_{n\times1}$, $Q_{n\times1}$ and $\lambda_{m\times1}$:

$$\begin{aligned} q &= \Phi(Q) \quad (n \; equations) \\ Q &= J^T\lambda \quad (n \; equations) \\ x &= f(q) \quad (m \; equations) \end{aligned} \tag{6}$$

The above conditions can be seen to define a manifold of dimension m (the dimension of the task space) in the n-dimensional joint space, and as x changes, the solution q will change but will always belong to this manifold. Thus this point is the equilibrium point.

For a small displacement of Δx away from the current equilibrium point, the corresponding Δq for the new equilibrium point is to be shown by Mussa-Ivaldi and Hogan [8] to be

$$\Delta q = (K - \Gamma)^{-1} J^T (J(K - \Gamma)^{-1} J^T)^{-1} \Delta x \tag{7}$$

where $\Gamma_{jk} = \frac{\partial^2 f_i}{\partial q_j \partial q_k} \lambda_i$.

2.2 Gradient Projection Method

Equation (6) gives us the necessary conditions for the minimum artificial potential energy, and Equation (7) tells us how to extrapolate the result from a known equilibrium point. Alternatively, we may consider numerical methods to "search" for the minimum potential energy solution suggested by Equation (4). We first discuss a simple numerical technique that uses a gradient based approach [7] to find the minimum. This technique lends itself to an implementation as a control law in which the manipulator finds the optimal configuration by following a suitable gradient. Consider the manipulator in

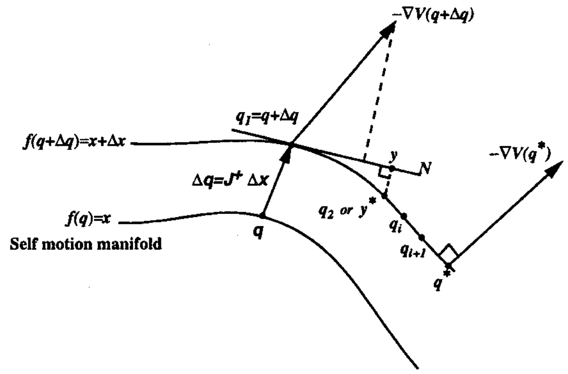

Figure 2: Gradient projection method.

a position of equilibrium so that x is the end-effector position and orientation and q is the current joint configuration. Suppose a new end-effector position, x_d, is specified. Let the new position be Δx away from the current position. In other words, $x_d = x + \Delta x$. We propose a two-step process to find the new joint configuration. See Figure 2.

1. We first use a simple pseudo-inverse technique to solve for the joint displacement, Δq, such that $f(q+\Delta q) = x + \Delta x$. In other words,

$$\Delta q = J^+ \Delta x \tag{8}$$

   The new joint position is given by q_1 in Figure 2.

2. Use a gradient-based method to move along the $f(q+\Delta q) = x_d$ contour while minimizing the potential energy:

$$\Delta q = -P\nabla V \tag{9}$$

   where $P = (I - J^T[JJ^T]^{-1}J)$ is the projection matrix onto the self-motion manifold, and I is a $n \times n$ identity matrix.

   Continue incrementing the joint position according to the above equation until Δq is very small. This will take us from q_1 to q_2 and so on until we eventually reach q^* at which the gradient of the potential energy will be normal to the self-motion manifold.

This two-step process guarantees the convergence to a local minimum of the potential energy while ensuring that the end-effector reaches the desired configuration.

Let us group Δq into two parts as:

$$\Delta q = \Delta q^+ + \Delta q_s \tag{10}$$

Here we use Δq^+ and Δq_s to denote components coming from the pseudo-inverse solution and the gradient search solution along the self-motion manifold respectively. As time-steps decrease, we can have the following control algorithm:

$$\dot{q} = J^+\dot{x} - P\nabla V(q) \tag{11}$$

This control law results in a steady state that is the same point that we get by using Equation (7) in the previous section.

3 Obstacle Modeling

Under the framework proposed in the previous section, obstacle avoidance can be integrated with the control algorithm by adding artificial fields which models the interactions between obstacles and links to V in Equation (11). On of the most well-known artificial potential fields which will serve this purpose is electric field.

According *Coulomb's law* [10], the electric attraction or repulsion between two point charges is directly proportional to the product of the charges and inversely proportional to the square of the distance between the points. It can be expressed as:

$$F = k\frac{c_1 c_2}{r^2}, \tag{12}$$

where k is a positive proportionality constant. The numerical value of k depends on the units in which F, c_1, c_2, and r are expressed. If c_1 and c_2 carry the same polarity of charges, then the interaction is repulsion, otherwise it is attraction. This force will get to infinity as distance r approaches zero. Since we want

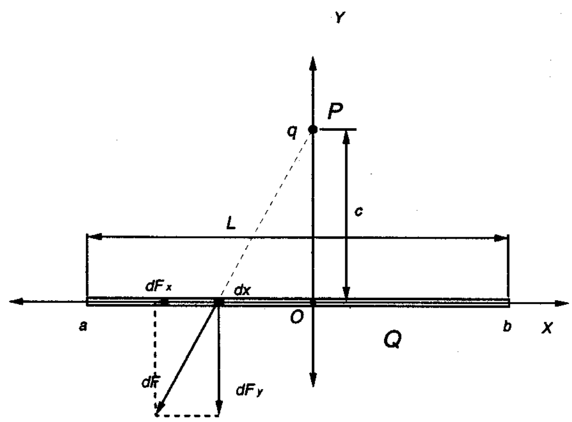

Figure 3: The electric forces between a point charge and a line charge.

to avoid collisions between the manipulator links and the obstacles, we need to give the manipulator links the same polarity as that of the obstacles. Consider the example of a manipulator link of length L near a point obstacle. Model the link as a line of length L, carrying a total charge of Q. It interacts with point P which carries a total charge of q. The force and couple acting on the line from the point charge can be found by integrating the interaction between P and a small segment dx of the line over the entire length of the line. The resultant force component along x and y axes, and the couple can be expressed as [10]:

$$F_x = \frac{kQq}{L}\left(\frac{1}{\sqrt{a^2+c^2}} - \frac{1}{\sqrt{b^2+c^2}}\right) \quad (13)$$

$$F_y = \frac{kQq}{L}\left(\frac{a}{\sqrt{a^2+c^2}} - \frac{b}{\sqrt{b^2+c^2}}\right) \quad (14)$$

$$M_O = \frac{kQq}{L}\left(\frac{c}{\sqrt{a^2+c^2}} - \frac{c}{\sqrt{b^2+c^2}}\right) \quad (15)$$

The effect of F_x, F_y and M_O can be replaced by a equivalent force $F = F_x + F_y$ applying at $d = \frac{M_O}{F_y}$ away from origin O. Furthermore, this external force can be projected into joint space as follows:

$$Q_{ij} = J_{Pj} F_{ij} \quad (16)$$

where the subscript i and j denotes the ith obstacle and jth link respectively. Because F_{ij} will not project any component onto joints after jth link, Jacobian J_{Pj} contains only the first j links. Adding all these joint forces to Δq_s in Equation (10), the repulsive forces will prevent manipulator links from colliding into obstacles.

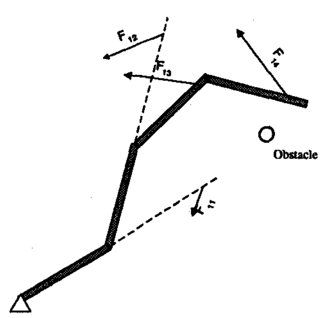

Figure 4: Repulsive force on each link.

4 Obstacle Avoidance

Figure 5 shows a 20 degree-of-freedom planar hyper-redundant manipulator. In this section, we are going to use this hyper-redundant manipulator as a platform to test if our control algorithm can tackle with typical obstacle avoidance problems. The real-time simulation is done on a Pentium 133 PC Linux and using Xwindow as its graphics interface.

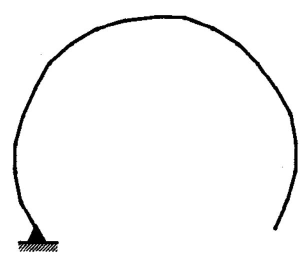

Figure 5: A 20 degree-of-freedom planar hyper-redundant manipulator.

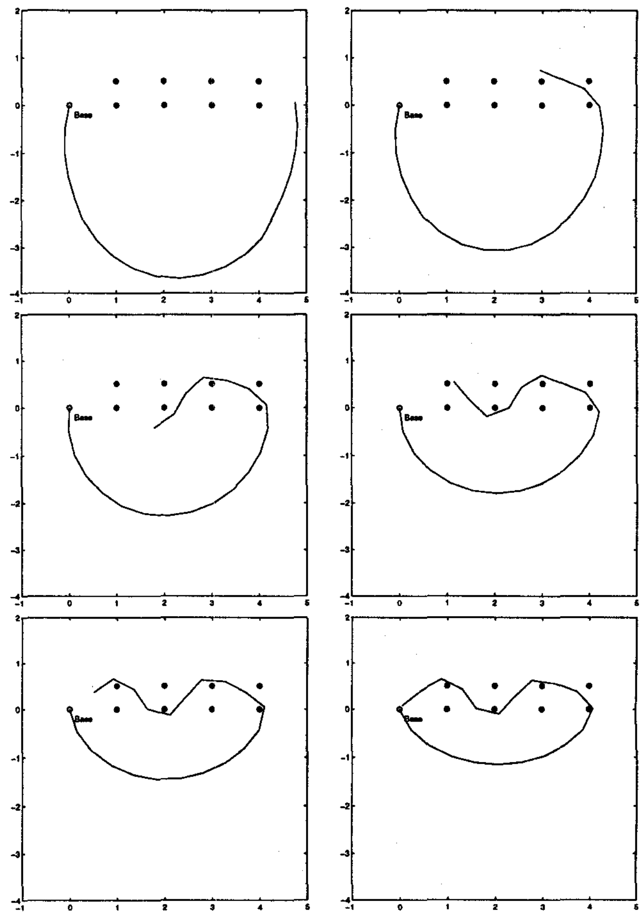

Figure 6: Obstacle avoidance of a 20-link hyper-redundant manipulator in a clustered workspace.

Example 1

Obstacle avoidance can get difficult if the workspace is full of objects. Here we command the hyper-redundant manipulators to "wiggle" around eight obstacles and come back to reach the base point. In this simulation, all links are of half unit long, and obstacles are one unit apart in horizontal direction and halt unit apart in vertical direction. Electric fields are constructed with unit point charge for obstacles, and unit line charge for links. Figure 6 shows how the manipulator end-effector can bend itself around obstacles. In the figure some links seem to collide into obstacles, but actually it does not. Because the point obstacles are made larger in size to be visible on the plot.

Example 2

When we model point obstacles, we do not explicitly specify whether the obstacles are stationary or in motion. Therefore, this algorithm can not tell whether the obstacles are moving or not. Here we let the hyper-redundant manipulator's end-effector remain fixed. A object approaches from the right-hand side. Without lowering the "hump" of the manipulator, a collision is sure to happen. But we can see from Figure 7 that the manipulator is pushed down by the repulsive force as the object approaches and moves back to where it was after the object is moving further away.

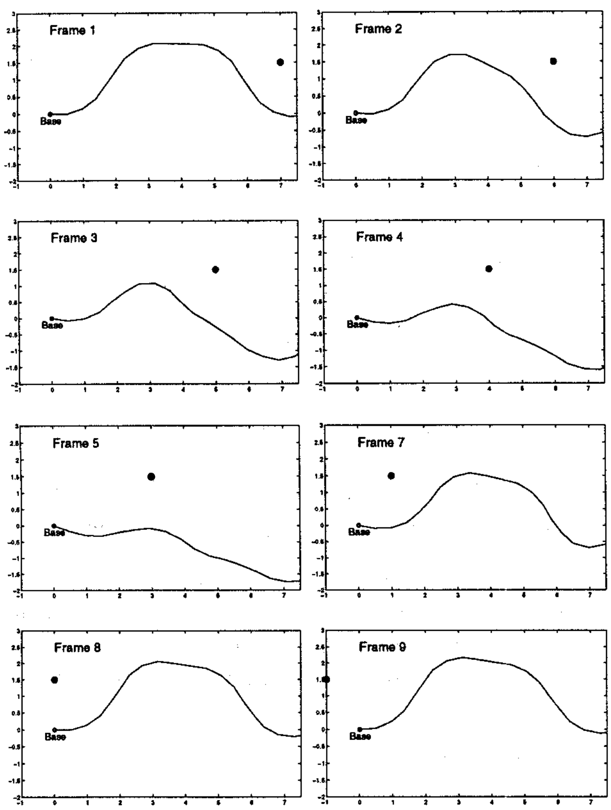

Figure 7: Obstacle avoidance with a moving object.

Example 3

Even though collision with point obstacles can be well avoided, it is still too simplified to apply them in real world. To overcome this limitation, we need to further model obstacles as line charges or even plan charges. Our preliminary study reveals that it is possible to model obstacles as line-charges, and the same control algorithm can be used without much major modification. But unlike the case of point charge obstacles versus line-charge links in Equation (14-15), line-charge obstacles versus line-charge links can be very complicated, and

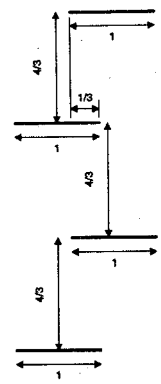

Figure 8: Dimension of the obstacle

one equation can occupy a half page. We will present the result in another paper. In Figure 9, a 10-link hyper-redundant is commanded to get through a corridor (its dimension is described in Figure 8.)

5 Discussion and Conclusion

Electric charges that we assign to links and obstacles do not dominate the repulsing behavior alone. It is also influenced by the stiffness we model for each manipulator joints. In other words, the absolute magnitude of electric charges or stiffness is not important. But what really matters is the ratio of energy accumulated in these two systems and the complicated kinematic conditions. One aspect of looking this approach is to investigate the physical significance of the parameters. For example, increase of obstacles' charge may correspond to have a larger clearance between links and obstacles. On the other hand, to simulate such a physical system with higher energy level, we need to use finer step size. This implies real-time simulation may not be feasible. Therefore design of electric charge is worth of further studies.

Moreover, as more potential fields being added to the system to model obstacles, the repeatability of kinematic solutions will be not guaranteed. Because more local minima will be created to divide the workspace and joint space such that there might not be a path between two given points without passing through singularities [11]. This paper proposes a gradient search algorithm to replace the linearized impedance-based control derived by Mussa-Ivaldi and Hogan [8]. By doing this, we can model obstacles and manipulator links with electric charges of the same polarity, and integrate these artificial fields into our gradient search algorithm. Obstacle avoidance can be achieved or guaranteed with knowledge that two charges of the same polarity can not get infinite close. Efficacy of this approach is demonstrated with 10-link and 20-link hyper-redundant manipulators carrying out obstacle avoidance in different workspace scenarios.

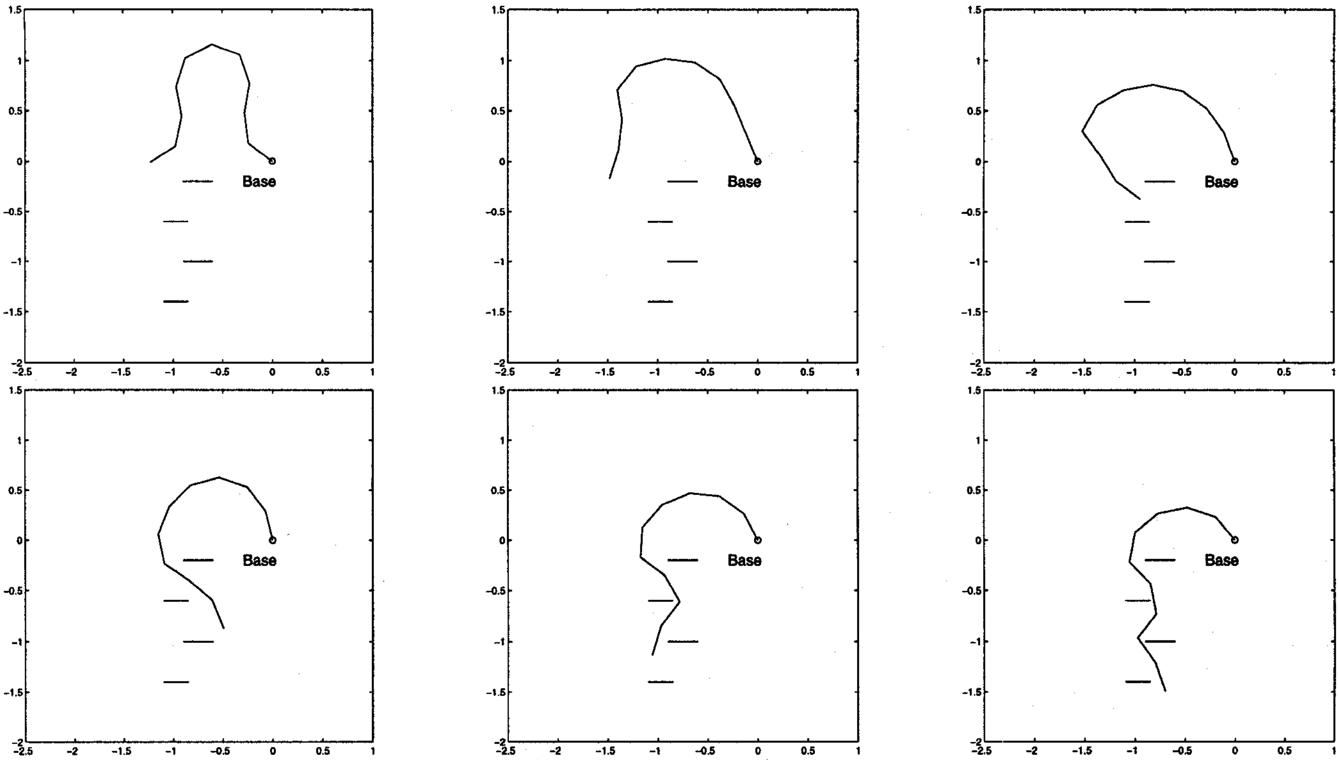

Figure 9: Obstacle avoidance in a corridor.

References

[1] J. Baillieul. Avoiding Obstacles and Resolving Kinematic Redundancy. In *Proc. International Conference on Advanced Robotics*, pages 1698–1704, San Fransisco, CA, 1986.

[2] R. Brooks. Solving the find-path problem by a good representation of free space. *IEEE Sys., Man Cyber*, SMC-13:190–197, 1983.

[3] G. Chirikjian and J. Burdick. An Obstacle Avoidance Algorithm for Hyper-Redundant Manipulator. In *Proceedings of 1990 International Conference on Robotics and Automation*, Cincinnati, OH, May 1990.

[4] O. Khatib. Real-Time Obstacle Avoidance for Manipulators and Mobile Robots. *International Journal of Robotics Research*, 5(1):90–99, 1986.

[5] P. Khosla and R. Volpe. Superquadric Artificial Potentials for Obstacle Avoidance and Approach. In *Proceedings of IEEE International Conference on Robotics and Automation*, pages 1778–1784, Philadelphia, PA, 1988.

[6] J. Kim and K. Khosla. Real-Time Obstacle Avoidance Using Harmonic Potential Functions. *IEEE Transactions on Robotics and Automation*, pages 338–349, June 1992.

[7] David G. Kuenberger. *Linear and Nonlinear Programming.* Addison Welsey, 1984.

[8] F. Mussa-Ivaldi and N. Hogan. Integrable Solution of Kinematic Redundancy via Impedance Control. In *International Journal Robotics Research*, pages 481–491, 1989.

[9] T. Nakamura, H. Hanafusa, and T. Yoshikawa. Task-Priority Based Redundancy Control of Robot Manipulators. *The International Journal of Robotics Research*, 6(2):3–15, 1987.

[10] F. W. Sears, M. W. Zemansky, and H. D. Young. *College Physics.* Addison-Wesley Publishing Company, 1985.

[11] C-C. Wang and V. Kumar. The Performance of Repeatable Control Schemes for Redundant Robots. In *Proceedings of 1995 International Conference on Robotics and Automation*, pages 1154–1159, 1995.